Fabrication of a nanofibrous scaffold with improved bioactivity for culture of human dermal fibroblasts for skin regeneration

2011 Biomed. Mater. 6 015001

(http://iopscience.iop.org/1748-605X/6/1/015001)

Biomed. Mater. **6** (2011) 015001 (10pp) doi:10.1088/1748-6041/6/1/015001

Fabrication of a nanofibrous scaffold with improved bioactivity for culture of human dermal fibroblasts for skin regeneration

Arun Richard Chandrasekaran[1,2], **J Venugopal**[1,3], **S Sundarrajan**[1] **and S Ramakrishna**[1]

[1] Healthcare and Energy Materials Laboratory, Nanoscience and Nanotechnology Initiative, Faculty of Engineering, National University of Singapore, Singapore
[2] Department of Chemistry, New York University, NY, USA

E-mail: nnijrv@nus.edu.sg

Received 25 June 2010
Accepted for publication 29 September 2010
Published 5 January 2011
Online at stacks.iop.org/BMM/6/015001

Abstract

Engineering dermal substitutes with electrospun nanofibres have lately been of prime importance for skin tissue regeneration. Simple electrospinning technology served to produce nanofibrous scaffolds morphologically and structurally similar to the extracellular matrix of native tissues. The nanofibrous scaffolds of poly(L-lactic acid)-co-poly(ε-caprolactone) (PLACL) and PLACL/gelatin complexes were fabricated by the electrospinning process. These nanofibres were characterized for fibre morphology, membrane porosity, wettability and chemical properties by FTIR analysis to culture human foreskin fibroblasts for skin tissue engineering. The nanofibre diameter was obtained between 282 and 761 nm for PLACL and PLACL/gelatin scaffolds; expressions of amino and carboxyl groups and porosity up to 87% were obtained for these fibres, while they also exhibited improved hydrophilic properties after plasma treatment. The results showed that fibroblasts proliferation, morphology, CMFDA dye expression and secretion of collagen were significantly increased in plasma-treated PLACL/gelatin scaffolds compared to PLACL nanofibrous scaffolds. The obtained results prove that the plasma-treated PLACL/gelatin nanofibrous scaffold is a potential biocomposite material for skin tissue regeneration.

(Some figures in this article are in colour only in the electronic version)

1. Introduction

Tissue engineering has striven to recreate natural three-dimensional environment for better cell and tissue growth through biomimicry-inspired design of materials [1]. Co-ordination of cells with their substrate is critical for the successful regeneration of any tissue construct [2]. Current tissue engineering research is based on seeding cells onto porous biodegradable polymer matrices [3] which can serve as substrates for cell attachment and tissue formation both *in vivo* and *in vitro*. A primary factor is the availability of good biomaterials to serve as temporary matrices for tissue engineering. The material selected for this purpose should be porous to offer a channel for migration of host cells into the matrix and also biodegradable into non-toxic products after serving the function *in vivo* [3]. The surface texture, along with the nature of a biomaterial controls cell adhesion, proliferation, shape and function [4, 5]. As demand increases for more sophisticated scaffolds, materials are designed in such a way that they would perform a more active role in guiding tissue development [6, 7].

Nanofibrous scaffolds, with their high surface area and porosity, are desirable for high-density cell and tissue cultures. These scaffolds act as substrates for cells until they regenerate a new extracellular matrix (ECM) in the region and will also result in an efficient, compact organ and a rapid recovery process [8]. An important aspect of these efforts is to mimic

[3] Author to whom any correspondence should be addressed.

the fibrillar structure of the ECM, which provides essential guidance for cell organization, survival and function [9]. The nonwoven scaffolds of electrospun nanofibres resemble the collagen structure of the ECM, in which nanoscale multi-fibrils of collagen are composed into a three-dimensional network together with proteoglycans [10]. In addition, because of their large surface area-to-volume ratio and porous structure, nanofibres also help in cell adhesion, proliferation [11], migration [12] and differentiation [13].

Nanofibrous scaffolds for wound healing and skin tissue regeneration have been of concern lately. Tissue-engineered dermal substitutes act as supplementary dermal templates and improve wound healing [14]. The primary aim of tissue-engineered skin is to achieve complete wound closure and restore normal skin function. Successful skin graft outcomes require adherence to wounds, histocompatibility, control of fluid loss and infection, absence of antigenicity and toxicity, mechanical stability and compliance, cost-effectiveness and availability [15, 16]. Electrospun nanofibrous membranes have shown uniform adherence to the wound surface without any fluid accumulation [17, 18]. Moreover, nanofibrous scaffolds overlook the restrictions faced by living skin substitutes such as insufficient skin donor and concerns of transmittable diseases [19]. In recent times, electrospinning has been the oft-used method for manufacturing nanofibres of synthetic [20–23] and natural [24] polymers.

Previous reports of nanofibrous scaffolds for wound dressing include those of polyurethane [17], amorphous poly(D,L-lactic acid) (PDLA) and semi-crystalline poly(L-lactic acid) (PLLA) [21], silk fibroin [25] and polycaprolactone (PCL) [26]. The nanofibres of PCL/collagen were used for the preparation of artificial dermis [11, 27]. Researchers have attributed improved wound healing for seeding fibroblasts into a dermal substitute [28, 29] as dermal fibroblasts have the best characteristics in terms of phenotype and cell proliferation [30].

The current study focuses on the fabrication of nanofibres using poly(L-lactic acid)-co-poly(ε-caprolactone) (PLACL) and gelatin and their potential use as substrates for the culture of human dermal fibroblasts. Previous research on the culture of smooth muscle cells [31, 32] and endothelial cells [33, 34] have used PLACL, a synthetic copolymer of PCL and PLLA [35], because of its beneficial features like biodegradability and non-toxicity. Gelatin is a protein produced by the partial hydrolysis of collagen and contains the Arg-Gly-Asp (RGD)-like sequence which promotes cell adhesion, migration and forms a polyelectrolyte complex [36]. Previous studies have used collagen as a substrate for cell culture as it is easily degraded and resorbed by the body. However, the use of collagen requires a cross-linking agent and thus could lead to cytotoxicity [37]. Also, collagen has poor mechanical properties and occurs in composites such as collagen–glycosaminoglycans which deter skin regeneration [38]. Use of gelatin overcomes these problems, and in combination with a synthetic polymer like PLACL, gives a 'bioartifical polymer' with enhanced biocompatibility and chemical properties. This study involves the characterization of these nanofibres and analysis of cell growth and proliferation to determine the efficiency of skin tissue regeneration on these biocomposite polymer nanofibrous scaffolds.

2. Materials and methods

2.1. Materials

Dulbecco's Modified Eagle's Medium, foetal bovine serum (FBS), antibiotics and trypsin–EDTA were purchased from GIBCO Invitrogen, USA. Poly(L-lactic acid)-co-poly-(ε-caprolactone) (70:30, Mw 150 kDa) was obtained from Boehringer Ingelheim Pharma, GmbH & Co., Ingelheim, Germany. Porcine gelatin and 1,1,1,3,3,3-hexafluor-2-propanol (HFP) were purchased from Sigma-Aldrich, USA. Dichloromethane (DCM) was obtained from Merck (Germany) and *N, N*-dimethyl formamide (DMF) was purchased from Sigma-Aldrich (USA).

2.2. Electrospinning of nanofibrous scaffolds

The nanofibres of PLACL and PLACL–gelatin blend (PLACL-G) were prepared by the electrospinning process. The electrospinning solutions of PLACL and PLACL-G were prepared by dissolving PLACL in DCM/DMF (70:30) and PLACL–gelatin mixture (3:1) in HFP to form 10% (w/v) and were stirred overnight at room temperature. Electrospinning was done using a 3 ml standard syringe with a blunted 22-gauge needle, and the solution flow rate was controlled by a syringe pump (KDS 100, KD Scientific, Holliston, MA). Electrospinning of PLACL and PLACL-G was carried out at a flow rate of 0.75 ml h^{-1} and 1 ml h^{-1} and at an applied voltage of 19.5 kV and 17.5 kV (Gamma High Voltage Research, USA), respectively. The solution flowing from the tip of the needle was splayed as nanofibres as a result of the charge density and was collected on coverslips placed over a grounded aluminium collector at a distance of 12–13 cm from the needle tip. Electrospinning conditions were maintained at 30 °C and 30% humidity. The membranes were dried under vacuum at room temperature overnight.

2.3. Characterization of nanofibrous scaffolds

The electrospun nanofibres were sputter-coated with gold (JEOL JFC-1200 Fine Coater, Japan) and visualized using a field emission scanning electron microscope (FESEM) (JEOL JSM 6700, Japan). The average diameter of the nanofibres was obtained using image analysis software (Image J, National Institute of Health, USA). Functional group characterization of PLACL and PLACL-G nanofibres was done by Fourier transform infrared (FTIR) spectroscopic analysis on Avatar 380 (Thermo Nicolet, Waltham, MA, USA) over a range of 500–3800 cm^{-1} at a resolution of 2 cm^{-1}. The wet-up/dry-up method of capillary flow porometer (CFP-1200-A, Ithaca, NY, USA) was used to measure the pore size of the nanofibrous scaffolds; the automated CFP system software was used for analysis of the pore size distribution. The thickness of nanofibrous scaffolds was measured using a micrometer and their porosity was calculated according to Ma *et al* [39].

Sessile drop water contact angle measurement (VCA Optima Surface Analysis system, AST products, Billerica, MA) was done to study the hydrophilic nature of the electrospun nanofibrous scaffolds. Air plasma treatment was done by an electrodeless radio frequency glow discharge plasma cleaner (PDC-001, Harrick Scientific Corporation, USA) for 2 min under vacuum at a radio frequency power of 30 W. The scaffolds were tested for their mechanical strength using a tabletop tensile tester (Instron 3345, USA) using a load cell of 10 N capacity. The membranes were cut into rectangular strips of 10 mm × 20 mm dimensions and mounted vertically on the gripping unit of the tester. Testing was done at a crosshead speed of 10 mm min^{-1} with data being recorded every 50 ms. The temperature was maintained at 18 °C and the humidity at 50%. Tensile stress, strain and elastic modulus were calculated based on the obtained tensile stress–strain curve.

2.4. Fibroblasts culture and proliferation

2.4.1. Fibroblasts culture. Human foreskin fibroblasts were purchased from American Type Culture Collection (ATCC, Manassas, VA, USA). The fibroblasts were cultured in DMEM supplemented with 10% foetal bovine serum (FBS) and 1% antibiotic and antimycotic solutions (Invitrogen Corp., USA) in a 75 cm^2 tissue culture flask and incubated at 37 °C in a humidified atmosphere with 5% CO_2. The populations of fibroblast passage 5 were used for this experiment. The electrospun scaffolds on coverslips were UV-sterilized, rinsed in phosphate-buffered saline (PBS) and soaked in cell culture medium overnight prior to cell seeding to facilitate protein adsorption and cell attachment. The fibroblasts were separated by trypsinization, centrifuged, counted using a haemocytometer and seeded on the scaffolds at a cell density of 1×10^4 cells/well and incubated at conditions suitable for cell growth. Tissue culture polystyrene (TCP) was used as the control for cell culture studies.

2.4.2. Cell proliferation. The proliferation of cultured fibroblasts was monitored on the third, sixth and ninth day of culture using the colorimetric MTS assay (CellTiter 96® AQ_{ueous} One solution, Promega, Madison, WI, USA). MTS (3-{4,5-dimethylthiazol-2-yl}-5-{3-carboxymethoxyphenyl}-2-{4-sulfophenyl}-2H-tetrazolium, inner salt) has a yellow tetrazolium salt which is reduced by the dehydrogenase enzymes secreted by metabolically active cells to form purple formazan crystals. The amount of formazan crystals formed varies proportionally with the number of cells. The samples were prepared for the MTS assay by rinsing with PBS to remove nonadherent cells and then incubated in a serum-free medium containing 20% MTS reagent for 3 h at 37 °C. After incubation, the samples were transferred to 96-well plate and their absorbance was read in a spectrophotometric plate reader (FLUOstar OPTIMA, BMG Lab Technologies, Germany) at 492 nm.

2.4.3. Expression of CMFDA dye. Fluorescent dye expression was observed in fibroblasts using CMFDA (5-chloromethylfluorescein diacetate), which on cleavage of its acetates by cytosolic esterases produces a brightly fluorescent CMFDA derivative. The cell culture medium was removed, followed by the addition of 180 μl of DMEM and 20 μl CMFDA (25 μM) to the cells adhered on the scaffolds and incubation at 37 °C for 2 h. The CMFDA medium was replaced by adding complete medium and cells were incubated overnight in the incubator. Then the culture medium was removed and the cells washed with PBS and, after addition of serum-free medium, observed under an inverted Leica DM IRB laser scanning microscope (Leica DC 300F) at 488 nm.

2.4.4. Expression of collagen. Sirius Red staining method was used for analysing the presence of collagen in the cell matrix. It is a strong anionic dye whose sulfonic acid groups interact with the basic groups of collagen staining it red. This helped us to determine the secretion of the collagen-containing ECM by fibroblasts in culture. The cells were first fixed with 10% formaldehyde, stained with Harris haematoxylin to distinguish the nucleus of the cells and washed three times with deionized water. This was followed by staining with Sirius red stain consisting of 0.1% Sirius red F3B in a saturated aqueous solution of picric acid for 1 h. The cells were washed with mild acidified water followed by 100% ethanol and viewed under a Leica BM IRB microscope. Collagen is stained red on a yellow background in the nanofibrous scaffolds.

2.5. Morphology of fibroblasts on scaffolds

A morphological study of *in vitro*-cultured fibroblasts was performed after 9 days of cell culture by processing them for SEM studies. After removal of non-adherent cells, the scaffolds with cells were fixed in 3% glutaraldehyde for 3 h followed by rinsing with deionized water. The cell–scaffolds samples were dehydrated using increasing concentrations of ethanol (50%, 70%, 90%, 100%), finally treated with hexamethyldisilazan and air-dried overnight to maintain normal cell morphology. Dried cellular constructs were sputter-coated with gold and observed under an FESEM at an accelerating voltage of 10 kV.

2.6. Statistical analysis

The data presented are expressed as mean ± standard deviation. Statistical analysis was done using Student's *t*-test and the significance level of the data was obtained. A *P*-value <0.05 was considered to be statistically significant.

3. Results and discussion

3.1. Morphology of nanofibrous scaffolds

The surface morphology of the nanofibre membranes was analysed by scanning electron microscopy. Images revealed that the membranes were beadless, porous structures of randomly aligned fibres (figure 1). The average fibre diameter of PLACL and PLACL-G nanofibres were in the range of

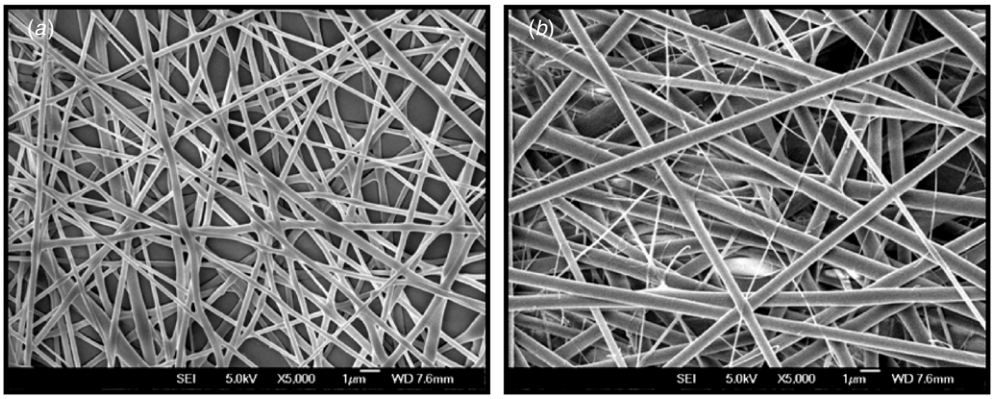

Figure 1. FESEM images of electrospun nanofibres: (*a*) PLACL, (*b*) PLACL-G.

Table 1. Characterization of nanofibrous scaffolds.

	Contact angle	Average fibre diameter (nm)	Mean flow pore diameter (μm)	Bubble point pore diameter (μm)
PLACL	121°	282 ± 53	0.457	1.118
PLACL-P	0°	273 ± 61	0.688	2.493
PLACL-G	129°	761 ± 97	1.376	2.385
PLACL-G-P	0°	727 ± 90	1.246	2.177

282 ± 53 nm and 761 ± 97 nm, respectively (table 1). The fibre diameters of PLACL-G in HFP would be expected to be low because of high solvent conductivity but the concentration of gelatin and the solution viscosity resulted in fibres with diameters in the higher nanometre range [40]. However, PLACL-G fibres were interspersed with thin fibres, which are due to the addition of gelatin. The surface roughness of these nanofibrous scaffolds is desirable for better cell attachment, growth and proliferation [41, 42] and is enhanced by the presence of functional groups and surface hydrophilicity [43]. The surface topography of nanofibres can be controlled by the electrospinning process to increase or decrease the fibre diameter and by the production of random or aligned fibres.

3.2. Wettability of nanofibres

Blending of synthetic and natural polymers imparts functional groups such as amine, hydroxyl and carboxyl groups to the scaffolds thereby improving their hydrophilic properties. This is important, as scaffolds with hydrophilic surfaces are better suited for cell adhesion and growth [44]. The contact angles obtained for PLACL and PLACL-G scaffolds were 121° and 129°, respectively, which imply that these scaffolds are highly hydrophobic and non-adsorbent to water. An increase in the concentration of gelatin in the PLACL-G blend has been reported to result in more hydrophilic characteristics [40]. Plasma treatment produces polar groups on the surfaces of the nanofibrous membranes, thus modifying the surface energy and increasing its reactivity with water [15]. The process induced complete wettability to both the nanofibrous membranes (plasma-treated samples: PLACL-P and PLACL-G-P), as confirmed by a contact angle of 0° with water. Kim *et al* report that the use of gelatin in electrospun nanofibres has a water uptake capacity of up to 417% which enhances the scaffolds ability to support cell growth [45]. A comparison between the fibre properties of PLACL and PLACL-G is illustrated in table 1. Gelatin is frequently used in hydrocolloid wound dressings and it has been shown that despite their high water retention, these occlusive dressings are less likely to become infected [46]. The rate of water uptake is directly related to the hydrophilic property of scaffolds and also helps to prevent dehydration and exudates build-up on the wounds [47].

3.3. Pore size distribution

The pore size of the nanofibrous scaffolds ranged from 0.1 to 2.5 μm and 0.4 to 2.4 μm for PLACL and PLACL-G respectively with an average pore diameter as shown in table 1. This is a desirable range since larger pore size enhances the cell supporting capacity of the membrane by increasing cell migration and nutrient flow [48]. The porosity of the scaffolds was calculated to be 84% and 87% for PLACL and PLACL-G respectively showing that the scaffolds were highly porous with fine fibres imparting a large surface area to the membranes (figure 2). This characteristic feature of nanofibrous membranes provides more room for cell adhesion and also helps in cell migration. Tissue engineering scaffolds require porosity as high as 90% to facilitate nutrient and metabolic waste flow and to provide room for new ECM regeneration. The difference in the pore diameters of PLACL and PLACL-G may have arisen because of the larger fibre diameter of PLACL-G which in turn affects the pore size. A decrease in pore diameter could be the result of a decrease in the fibre diameter of the nanofibres [49].

3.4. Mechanical properties

PLACL and PLACL-G scaffolds showed a typical nonlinear stress–strain curve as illustrated in figure 3. The tensile

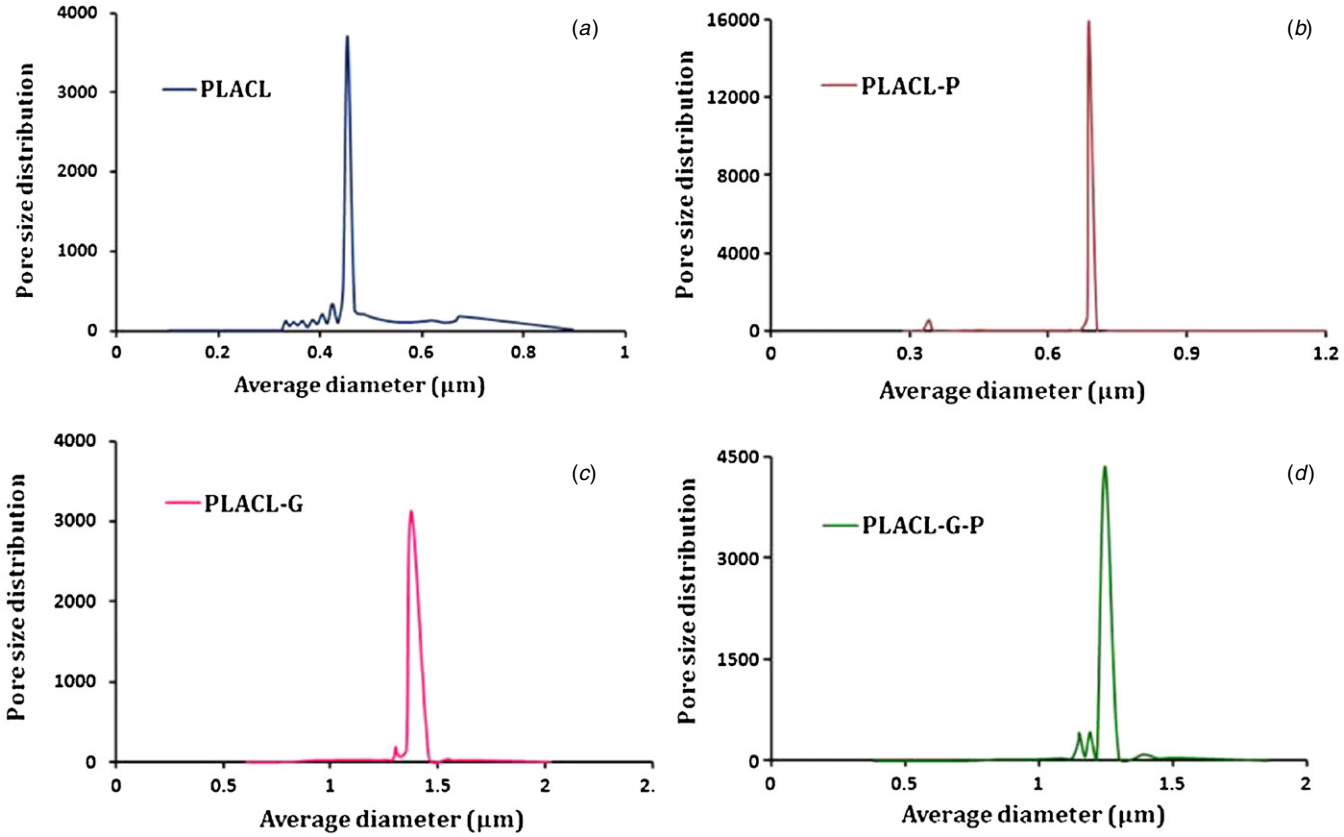

Figure 2. Pore size distribution curves of nanofibrous scaffolds: (*a*) PLACL, (*b*) PLACL-P, (*c*) PLACL-G, (*d*) PLACL-G-P.

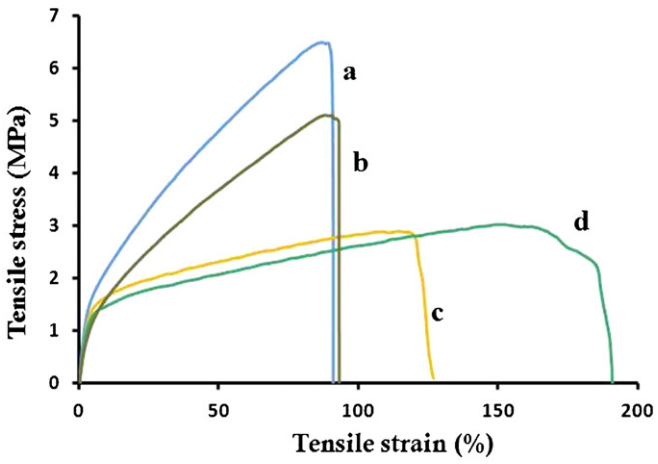

Figure 3. Tensile stress–strain characteristics of nanofibrous scaffolds: (*a*) PLACL, (*b*) PLACL-P, (*c*) PLACL-G and (*d*) PLACL-G-P nanofibres.

stress obtained for PLACL was 6.50 MPa and 5.11 MPa for PLACL-P. In the case of PLACL-G blend, the tensile stress was 2.88 and 3.02 MPa for PLACL-G and PLACL-G-P, respectively. The tensile properties of PLACL-G (3:1 wt%)-blended nanofibres were higher than that of PLACL nanofibres. An as-spun PLACL-G scaffold could bear a strain of 114.46% and 150.04% after plasma treatment. The strain endured by as-spun PLACL was 86.29% and by

Table 2. Tensile properties of electrospun nanofibrous membranes.

	Tensile stress (MPa)	Tensile strain (%)	Tenacity (gf/tex)
PLACL	6.50	86.29	2.85
PLACL-P	5.11	88.08	1.72
PLACL-G	2.88	114.46	1.26
PLACL-G-P	3.02	150.04	2.16

PLACL-P was 88.08%. The results implied that blending PLACL with gelatin gives favourable mechanical properties to the nanofibrous scaffolds. The hydrated scaffolds of blended natural and synthetic polymers have been found to be more flexible because of the presence of gelatin. This gives them an advantage of acting as a support for cell adhesion and proliferation [45]. Addition of 10–39 wt% of gelatin has previously resulted in enhanced tensile properties of PLACL-G scaffolds [50]. The mechanical properties of PLACL and PLACL-G scaffolds are shown in table 2. The mechanical stability of the substrate plays an important role as the membrane should facilitate cell growth and proliferation and degrade by itself as new ECM starts regenerating. Very high tensile strength may result in the substrate staying with the wound bed long after regeneration, thus obstructing new tissue development, while a weaker membrane may not support cell growth for the required time period of tissue engineering.

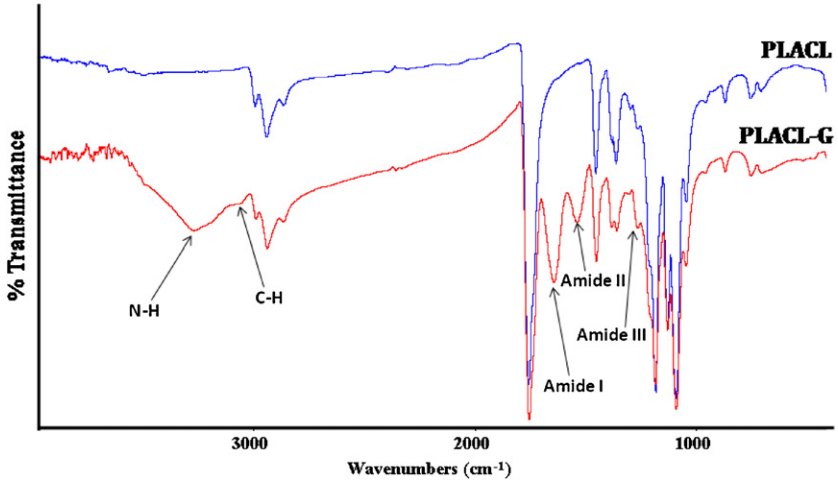

Figure 4. FTIR spectrum of PLACL and PLACL-G nanofibres.

3.5. FTIR analysis

The chemical characteristics of functional groups on the nanofibres were studied by FTIR (figure 4). The analysis showed the bands of N–H and C–H stretch at 3194 cm^{-1} and 3032 cm^{-1}, respectively. These form the characteristic peaks for gelatin and suggest the presence of amide groups on the surface of PLACL-G fibres. The amide I band of gelatin for the C=O stretch—the measure of secondary structure of proteins—was prominent at 1720 cm^{-1} in PLACL-G. The amide II peak for the N–H bend coupled with the C–N stretch was obtained at 1527 cm^{-1} and the amide III region for the N–H bend was observed between 1200 and 1250 cm^{-1}. The amide III region corresponds to the triple helix structure of gelatin which is structurally similar to collagen, the integral part of the ECM, and greatly favours cell adhesion and proliferation [51].

3.6. Expression of fluorescent dye and collagen

Interaction between cells and the scaffold material depends on the physical and chemical properties of the material and particularly on chemical composition, particle size and surface properties which include topography, roughness, surface energy and wettability [52]. The compound CMFDA belongs to a group of chloromethyl derivatives developed for labelling of living cells *in vitro* [53, 54]. The CMFDA compound is metabolized intracellularly in viable cells and converted to a cell-impermeant and fluorescent state within 1 h. The addition of CMFDA to the cell culture medium causes the compound to freely permeate the cell membrane and be acted upon by cytosolic esterases, producing a CMFDA derivative that is brightly fluorescent. Further, in a reaction thought to be mediated by glutathione S-transferase [55], this CMFDA derivative conjugates to intracellular thiols and becomes cell-impermeant. CMFDA dye expression was observed on the sixth and ninth day of fibroblast culture using a Leica fluorescence microscope. The fibroblast cells' density and morphology were observed to be better in PLACL-G plasma-treated scaffolds compared to other nanofibrous scaffolds (figure 5).

Collagen staining with Picro-sirius red confirmed the secretion of the ECM by the cells in culture. Figure 6 shows the secretion of collagen on fibroblasts grown on PLACL and PLACL-G nanofibrous scaffolds. The results showed that the secretion of collagen PLACL-G plasma-treated nanofibrous scaffolds was better than all other scaffolds. The secretion of collagen proves that the biocomposite nanofibrous scaffolds have potential for wound healing through skin tissue regeneration.

3.7. Cell proliferation and cell–scaffold interaction

PLACL-G plasma-treated nanofibrous scaffolds were more suitable for growth of fibroblasts as compared to PLACL scaffolds, attaining a significant level ($P < 0.05$) of increase in cell proliferation after day 6 and day 9 of culture and a percent level of increase up to 40% after day 9 of culture (figure 7). The percentages of cell proliferation increase on PLACL-P and PLACL-G were only 10% and 14%, respectively. Furthermore, a significant level of increase in proliferation ($P < 0.001$) was seen in PLACL-G-P showing that the fibres with gelatin assisted increased proliferation of the fibroblasts. A large number of interconnected pores and the rough surface of the nanofibrous membrane support the proliferation of fibroblasts and quicker regeneration of skin tissue [56]. In addition to the porous nature and suitable mechanical properties, molecular signals from the nanofibres may also guide cells entering the cell substrate by their amoeboid movement [37]. The hydrophilic nature of the PLACL-G scaffolds is another reason for better adhesion and proliferation of fibroblasts.

An increasing demand for organs and tissues has inspired scientists to dwell in tissue engineering research aiming to produce biological substitutes that overcome the limitations of conventional clinical treatments for damaged tissues or organs [57]. The SEM micrographs of fibroblasts on PLACL and PLACL-G-P scaffolds obtained on day 9 of culture showed a normal morphology of cell growth on the nanofibres (figure 8). Cell growth was higher on PLACL-G-P nanofibrous scaffolds

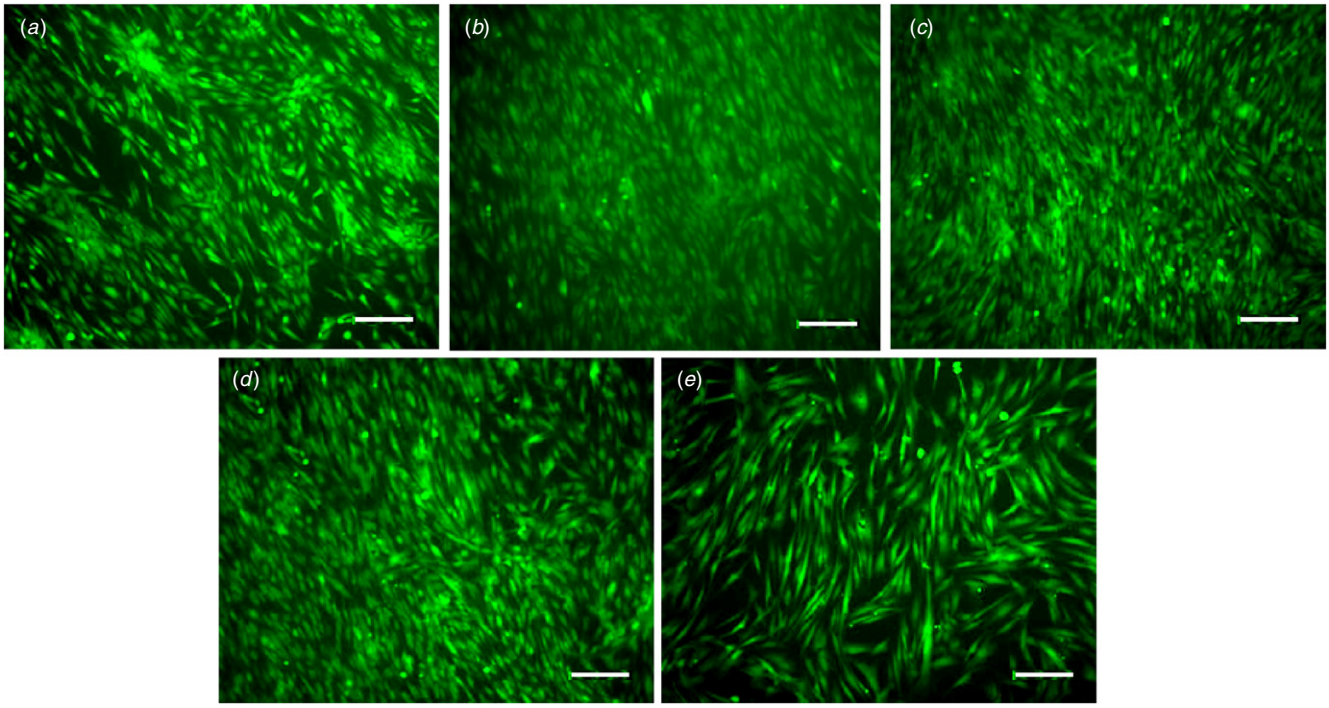

Figure 5. The detection of CMFDA-labelled fibroblasts on day 9 of cell culture: (*a*) PLACL, (*b*) PLACL-P, (*c*) PLACL-G, (*d*) PLACL-G-P and (*e*) TCP. Scale bar 100 μm.

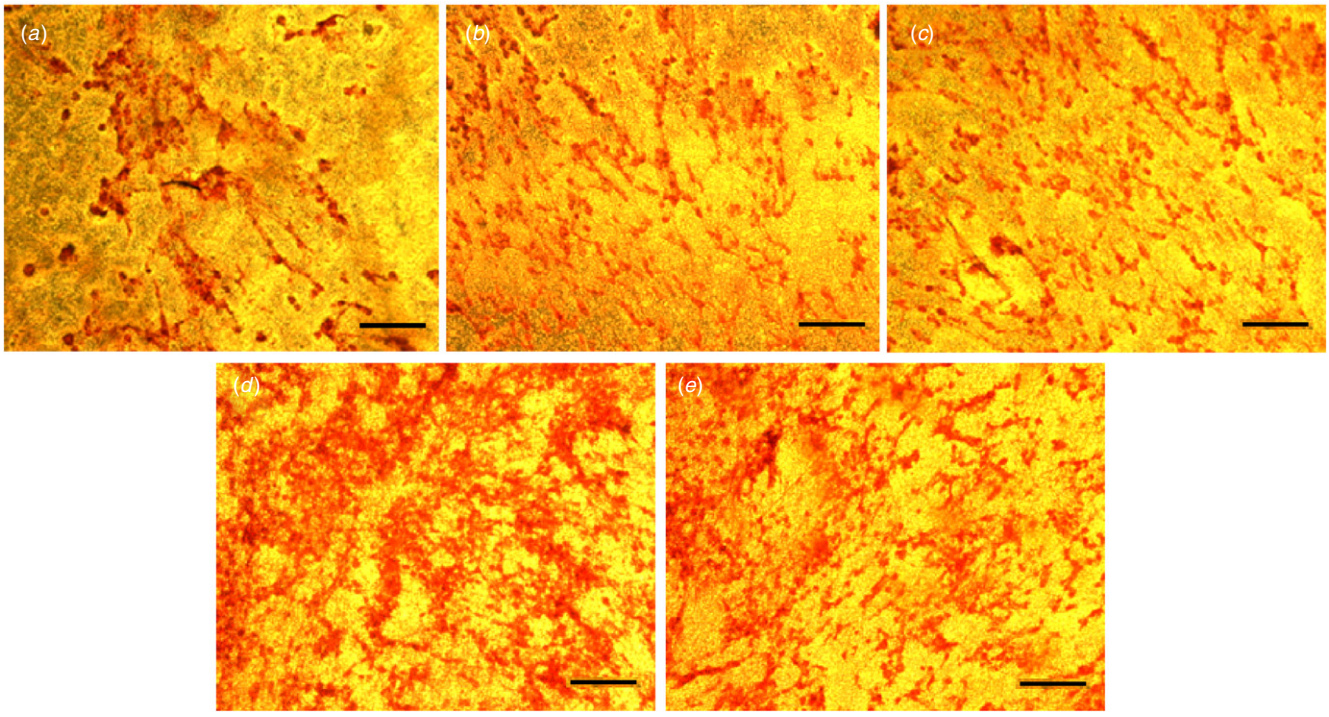

Figure 6. Collagen staining on fibroblasts on nanofibrous scaffolds: (*a*) PLACL, (*b*) PLACL-P, (*c*) PLACL-G, (*d*) PLACL-G-P and (*e*) TCP. Scale bar 100 μm.

than on PLACL nanofibres. Gelatin contains many integrin-binding sites similar to those found on collagen and these sites facilitate cell adhesion and differentiation. Increased cell adhesion on the nanofibre matrix is also attributed to adhesion proteins such as fibronectin and vitronectin present in the serum used for cell culture [58, 59]. PLACL, being a biocompatible, nontoxic, synthetic polymer, on blending with gelatin provides a scaffold with improved bioactivity and cell affinity for skin tissue regeneration.

Collagen is a natural polymer used for the fabrication of electrospun nanofibrous scaffolds for tissue engineering. The scaffolds used in this study provide the same requirements

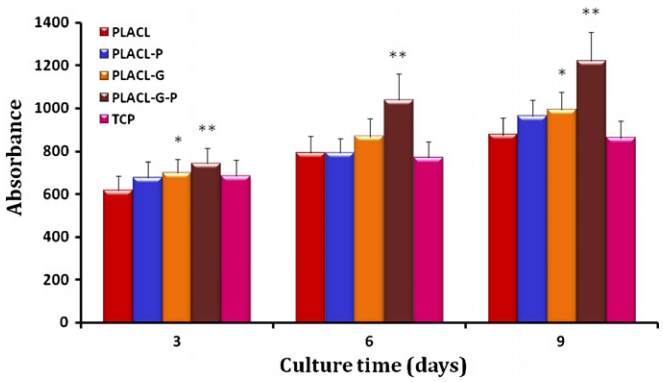

Figure 7. MTS assay for proliferation of fibroblasts on nanofibrous scaffolds and TCP. Bar represents mean standard deviation. Asterisks indicate the significant level of proliferation obtained by the *t*-test. $^{*}P < 0.05$, $^{**}P < 0.001$.

similar to collagen by blending gelatin into the electrospinning polymer solution. The chemical properties of gelatin which makes it a good cell adhesion substrate have already been discussed in this study for skin tissue engineering. The PLACL-G scaffolds in comparison with the previous scaffolds of PCL–collagen and PLLA will serve as better tissue engineering scaffolds in the longer run because of the relatively low cost and biological origin of gelatin in addition to its water retention properties which are typically required for light-to-moderate exudates wounds.

4. Conclusion

Tissue engineering scaffolds for skin tissue regeneration is an ever expanding area, as the products that meet the requirement are far and few. In future, better approaches would be to devise nanofibrous scaffolds which are capable of supporting the tissues in their natural environment and possess controlled surface topography as well as structural morphology. One such approach could be to formulate nonwoven 3D scaffolds for wound dressing and skin tissue regeneration. However, it is also essential to know what external and internal stimuli trigger the production of the ECM by the cells *in vitro*. This is important as ECM-like features—especially the morphological similarity to the ECM protein fibre network—of the scaffold will enhance cellular response and biocompatibility of the matrix [60]. In addition, tissue engineering matrices populated with autologous fibroblasts improve tissue regeneration and reduce wound contraction [61–63]. The observed results of PLACL-G-P nanofibrous scaffolds show sufficient porous structures and mechanical stability, and loose peripheral regions of the scaffold are favourable for cell infiltration and provide enough space for fibroblast ingrowth for the formation of a dermal substitute for skin tissue regeneration.

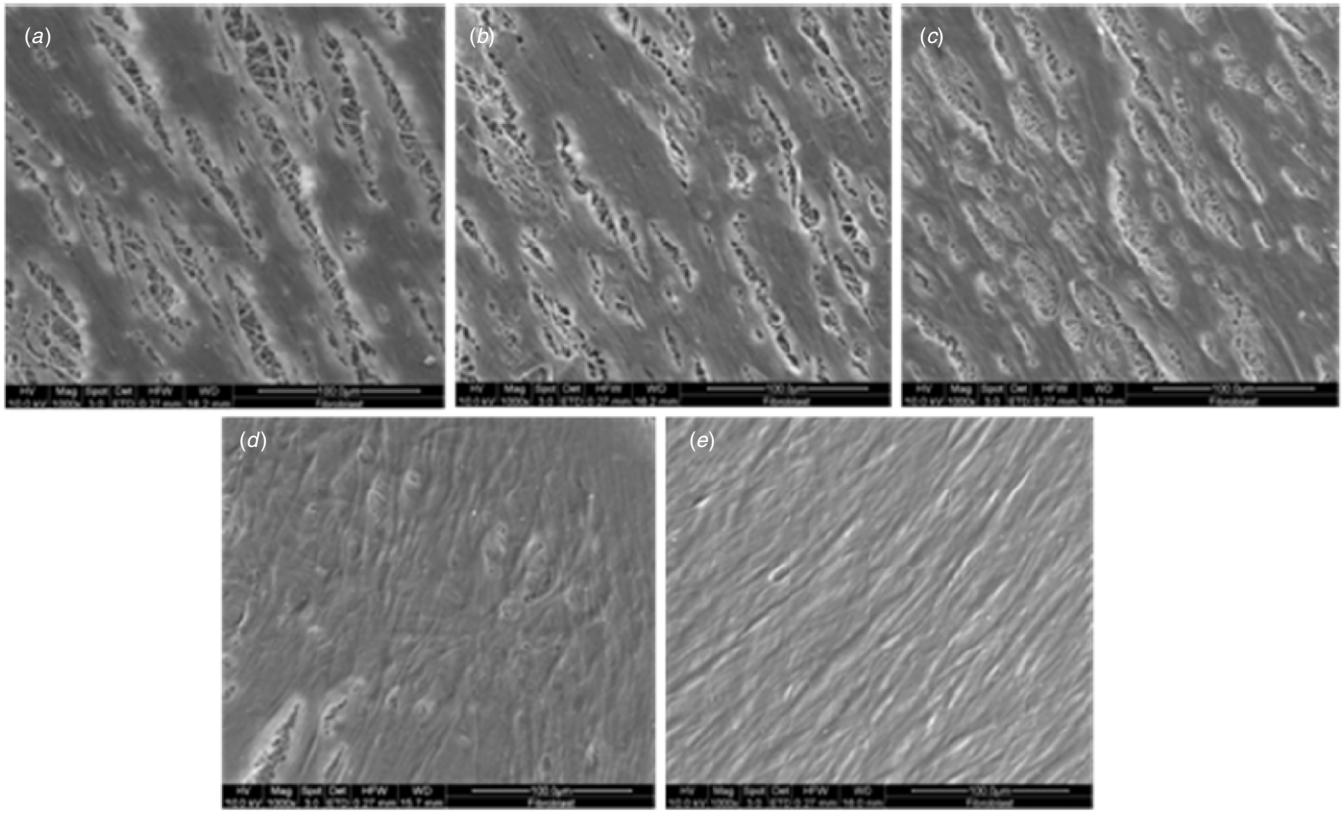

Figure 8. FESEM images of fibroblasts grown on nanofibrous scaffolds: (*a*) PLACL, (*b*) PLACL-P, (*c*) PLACL-G, (*d*) PLACL-G-P and (*e*) TCP.

Acknowledgments

This study was supported by the NRF-Technion (R-398-001-065-592), Ministry of Manpower (R-265-000-318-112) and NUSNNI, National University of Singapore, Singapore.

References

[1] Hubbell J A 2003 Materials as morphogenetic guides in tissue engineering *Curr. Opin. Biotechnol.* **14** 551–58
[2] Bonassar L J and Vacanti C A 1998 Tissue engineering: the first decade and beyond *J. Cell. Biochem. Suppl.* **30/31** 297–303
[3] Khor E and Lim L Y 2003 Implantable applications of chitin and chitosan *Biomaterials* **24** 2339–49
[4] Patel N, Padera R, Sanders G H, Cannizzaro S M, Davies M C, Langer R, Roberts C J, Tendler S J, Williams P M and Shakesheff K M 1998 Spatially controlled cell engineering on biodegradable polymer surfaces *FASEB J.* **12** 1447–54
[5] van Kooten T G, Whitesides J F and von Recum A F 1998 Influence of silicone (PDMS) surface texture on human skin fibroblast proliferation as determined by cell cycle analysis *J. Biomed. Mater. Res.* **B 43** 1–14
[6] Furnas D W, Achauer B M and Bartlett R H 1980 Reconstruction of the burned nose *J. Trauma* **20** 25–31
[7] Shakesheff K M, Cannizzaro S M and Langer R 1998 Creating biomimetic micro-environments with synthetic polymer-peptide hybrid molecules *J. Biomater. Sci. Polym. Ed.* **9** 507–18
[8] Frenot A and Chronakis I 2003 Polymer nanofibres assembled by electrospinning *Curr. Opin. Colloid Interface Sci.* **8** 64–75
[9] Zonga X, Bien H, Chung C-Y, Yin L, Fang D, Hsiao B S, Chu B and Entcheva E 2005 Electrospun fine-textured scaffolds for heart tissue constructs *Biomaterials* **26** 5330–38
[10] Nishida T, Yasumoto K, Ortori T and Desaki J 1988 The network structure of corneal fibroblasts in the rat as revealed by scanning electron microscopy *Invest. Ophthalmol. Vis. Sci.* **29** 1887–90
[11] Venugopal J R, Zhang Y Z and Ramakrishna S 2006 *In vitro* culture of human dermal fibroblasts on electrospun polycaprolactone collagen nanofibrous membrane *Artif. Organs* **30** 440–46
[12] Zhang Y Z, Ouyang H W, Lim C T, Ramakrishna S and Huang Z M 2005 Electrospinning of gelatin fibres and gelatin/PCL composite fibrous scaffolds *J. Biomed. Mater. Res.* B **72** 156–65
[13] Badami A S, Kreke M R, Thompson M S, Riffle J S and Goldstein A S 2006 Effect of fibre diameter on spreading, proliferation, and differentiation of osteoblastic cells on electrospun poly(lactic acid) substrates *Biomaterials* **27** 596–606
[14] van Zuijlen P P M, van Trier A J M, Vloemans J F P M, Groenevelt F, Kreis R W and Middelkoop E 2000 Graft survival and effectiveness of dermal substitution in burns and reconstructive surgery in a one-stage grafting model *Plast. Reconstr. Surg.* **106** 615–23
[15] Chen W Y J and Abatangelo G 1999 Functions of hyaluronan in wound repair *Wound Repair Regen.* **7** 79–89
[16] Miclau T, Edin M L, Lester G E, Lindsey R W and Dahners L E 1995 Bone toxicity of locally applied aminoglycosides *J. Orthop. Trauma* **9** 401–6
[17] Khil M-S, Cha D-I, Kim H-Y, Kim I-S and Bhattarai N 2003 Electrospun nanofibrous polyurethane membrane as wound dressing *J. Biomed. Mater. Res.* B **67** 675–79
[18] Bhattarai S R, Bhattarai N, Yi H K, Hwang P H, Cha D I and Kim H Y 2004 Novel biodegradable electrospun membrane: scaffold for tissue engineering *Biomaterials* **25** 2595–602
[19] Venugopal J, Prabhakaran M P, Low S, Choon A T, Zhang Y Z, Deepika G and Ramakrishna S 2008 Nanotechnology for nanomedicine and delivery of drugs *Curr. Pharm. Des.* **14** 2184–200
[20] Kim K, Yu M, Zong X, Chiu J, Fang D, Hsiao B S, Chu B and Hadjiargyrou M 2003 Control of degradation rate and hydrophilicity in electrospun non-woven poly(D,L-lactide) nanofibre scaffolds for biomedical applications *Biomaterials* **24** 4977–85
[21] Zong X, Kim K, Fang D, Ran S, Hsiao B S and Chu B 2002 Structure and process relationship of electrospun bioabsorbable nanofibre membranes *Polymer* **43** 4403–12
[22] Luu Y K, Kim K, Hsiao B S, Chu B and Hadjiargyrou M 2003 Development of a nanostructured DNA delivery scaffold via electrospinning of PLGA and PLA-PEG block copolymers *J. Control. Release* **89** 341–53
[23] Zong X, Ran S, Fang D, Hsiao B S and Chu B 2003 Control of structure, morphology and property in electrospun poly(glycolide-co-lactide) non-woven membranes via post-draw treatments *Polymer* **44** 4959–67
[24] Matthews J A, Wnek G E, Simpson D G and Bowlin G L 2002 Electrospinning of collagen nanofibres *Biomacromolecules* **3** 232–38
[25] Min B M, Lee G, Kim S H, Nam Y S, Lee T S and Park W H 2004 Electrospinning of silk fibroin nanofibres and its effect on the adhesion and spreading of normal human keratinocytes and fibroblasts *in vitro Biomaterials* **25** 1289–97
[26] Venugopal J and Ramakrishna S 2005 Applications of polymer nanofibres in biomedicine and biotechnology *Appl. Biochem. Biotechnol.* **125** 147–57
[27] Venugopal J, Ma L L and Ramakrishna S 2005 Biocompatible nanofibre matrices for the engineering of a dermal substitute for skin regeneration *Tissue Eng.* **11** 847–54
[28] Ojeh N O, Frame J D and Navsaria H A 2001 *In vitro* characterization of an artificial dermal scaffold *Tissue Eng.* **7** 457–72
[29] Coulomb B, Friteau L, Baruch J, Guilbaud J, Chretien-Marquet B, Glicenstein J, Lebreton-Decoster C, Bell E and Dubertret L 1998 Advantage of the presence of living dermal fibroblasts within *in vitro* reconstructed skin for grafting in humans *Plast. Reconstr. Surg.* **101** 1891–903
[30] van den Bogaerdt A J, van Zuijlen P P M, van Galen M, Lamme E N and Middelkoop E 2002 The suitability of cells from different tissues for use in tissue-engineered skin substitutes *Arch. Dermatol. Res.* **294** 135–42
[31] Mo X M, Xu C Y, Kotaki M and Ramakrishna S 2004 Electrospun P(LLA-CL) nanofibre: a biomimetic extracellular matrix for smooth muscle cell and endothelial cell proliferation *Biomaterials* **25** 1883–90
[32] Xu C Y, Inai R, Kotaki M and Ramakrishna S 2004 Aligned biodegradable nanofibrous structure: a potential scaffold for blood vessel engineering *Biomaterials* **25** 877–86
[33] He W, Yong T, Teo W E, Ma Z and Ramakrishna S 2005 Fabrication and endothelialization of collagen-blended biodegradable polymer nanofibres: potential vascular graft for blood vessel tissue engineering *Tissue Eng.* **11** 1574–88
[34] He W, Yong T, Inai R, Teo W E and Ramakrishna S 2006 Biodegradable polymer nanofibre mesh to maintain functions of endothelial cells *Tissue Eng.* **12** 2457–66
[35] Lemmouchi Y and Schacht E 1997 Preparation and *in vitro* evaluation of biodegradable poly(ε-caprolactone-co-D,L lactide)(*X*–*Y*) devices containing trypanocidal drugs *J. Control. Release* **45** 227–33

[36] Huang Y, Onyeri S, Siewe M, Moshfeghian A and Madihally S V 2005 *In vitro* characterization of chitosan-gelatin scaffolds for tissue engineering *Biomaterials* **26** 7616–27
[37] Venugopal J R, Low S, Choon A T, Kumar A B and Ramakrishna S 2008 Nanobioengineered electrospun composite nanofibres and osteoblasts for bone regeneration *Artif. Organs* **32** 388–97
[38] Wahl D A and Czernuszka J T 2006 Collagen–hydroxyapatite composites for hard tissue repair *Eur. Cell Mater.* **11** 43–56
[39] Ma Z W, Kotaki M, Yong T, He W and Ramakrishna S 2005 Surface engineering of electrospun polyethylene terephthalate (PET) nanofibres towards development of a new material for blood vessel engineering *Biomaterials* **26** 2527–36
[40] Gupta D, Venugopal J, Mitra S, Giri Dev V R and Ramakrishna S 2009 Nanostructured biocomposite substrates by electrospinning and electrospraying for the mineralization of osteoblasts *Biomaterials* **30** 2085–94
[41] Martinez E C, Ivirico J L E, Criado M I, Ribelles J L G, Pradas M M and Sanchez M S 2007 Effect of poly (L-lactide) surface topography on the morphology of *in vitro* cultured human articular chondrocytes *J. Mater. Sci., Mater. Med.* **18** 1627–32
[42] Yang F, Murugan R, Ramakrishna S, Wang X, Ma Y X and Wang S 2004 Fabrication of nano-structured porous PLLA scaffold intended for nerve tissue engineering *Biomaterials* **25** 1891–900
[43] Kwideok P, Young M J, Jun S S, Kwang-Duk A and Dong K H 2007 Surface modification of biodegradable electrospun nanofibre scaffolds and their interaction with fibroblast *J. Biomat. Sci. Polym. Ed.* **18** 369–82
[44] Gotoh Y, Hiraiwa K and Narajama M 1990 *In vitro* mineralization of osteoblastic cells derived from human bone *Bone Miner.* **8** 239–50
[45] Kim S E, Heo D N, Lee J B, Kim J R, Park S H, Jeon S H and Kwon I K 2009 Electrospun gelatin/polyurethane blended nanofibres for wound healing *Biomed. Mater.* **4** 044106
[46] Hutchinson J J and Lawrence J C 1991 Wound infection under occlusive dressings *J. Hosp. Infect.* **17** 83–94
[47] Zahedi P, Rezaeian I, Ranaei-Siadat S-O, Jafari S-H and Supaphol P 2010 A review on wound dressings with an emphasis on electrospun nanofibrous polymeric bandages *Polym. Adv. Technol.* **21** 77–95
[48] Agrawal C M and Ray R B 2001 Biodegradable polymeric scaffolds for musculoskeletal tissue engineering *J. Biomed. Mater. Res.* **55** 141–50
[49] Li D, Frey M W and Joo Y L 2006 Characterization of nanofibrous membranes with capillary flow porometry *J. Membr. Sci.* **286** 104–14
[50] Lee J, Tae G, Kim Y H, Park I S, Sang-Heon K and Kim S H 2008 The effect of gelatin incorporation into electrospun poly(l-lactide-co-caprolactone) fibres on mechanical properties and cytocompatibility *Biomaterials* **29** 1872–79
[51] Muyonga J H, Cole C G B and Duodu K G 2004 Fourier transform infrared (FTIR) spectroscopic study of acid soluble collagen and gelatin from skins and bones of young and adult Nile perch *Food Chem.* **86** 325–33
[52] Guo X, Gough J E, Xiao P, Liu J and Shen Z 2007 Fabrication of nanostructured hydroxyapatite and analysis of human osteoblastic cellular response *J. Biomed. Mater. Res.* A **82** 1022–32
[53] Poot M, Kavanagh T J, Kang H C, Haugland R P and Rabinovitch P S 1991 Flow cytometric analysis of cell cycle-dependent changes in cell thiol level by combining a new laser dye with Hoechst 33342 *Cytometry* **12** 184–87
[54] Zhang Y-Z, Olson N, Mao F, Roth B and Haugland R P 1992 New fluorescent probes for long-term tracing of living cells *FASEB J.* **6** A1835
[55] Zhang Y-Z, Naleway J J, Larison K D, Huang Z J and Haugland R P 1991 Detecting lacZ gene expression in living cells with new lipophilic, fluorogenic beta-galactosidase substrates *FASEB J.* **5** 3108–13
[56] Murugan R and Ramakrishna S 2007 Design strategies of tissue engineering scaffolds with controlled fibre orientation *Tissue Eng.* **13** 1845–66
[57] Venugopal J, Low S, Choon A T and Ramakrishna S 2008 Mineralization of osteoblasts with electrospun collagen/hydroxyapatite nanofibres *J. Mater. Sci., Mater. Med.* **19** 2039–46
[58] Anselme K 2000 Osteoblast adhesion on biomaterials *Biomaterials* **21** 667–81
[59] Grinnell F 1986 Focal adhesion sites and the removal of substratum-bound fibronectin *J. Cell Biol.* **103** 2697–706
[60] Li W J, Laurencin C T, Caterson E J, Tuan R S and Ko F K 2002 Electrospun nanofibrous structure: a novel scaffold for tissue engineering *J. Biomed. Mater. Res.* **60** 613–21
[61] de Vries H J, Middelkoop E, van Heemstra-Hoen M, Wildevuur C H and Westerhof W 1995 Stromal cells from subcutaneous adipose tissue seeded in a native collagen/elastin dermal substitute reduce wound contraction in full thickness skin defects *Lab Invest.* **73** 532–40
[62] Lamme E N, van Leeuwen R T J, Jonker A, van Marle J and Middelkoop E 1998 Living skin substitutes: survival and function of fibroblasts seeded in a dermal substitute in experimental wounds *J. Invest. Dermatol.* **111** 989–95
[63] Lamme E N, van Leeuwen R T J, Brandsma K, van Marle J and Middelkoop E 2000 Higher numbers of autologous fibroblasts in an artificial dermal substitute improve tissue regeneration and modulate scar tissue formation *J. Pathol.* **190** 595–603